Role of Micellar Equilibria on Modelling of Batch Emulsion Polymerization Reactors

MASSIMO MORBIDELLI, GIUSEPPE STORTI, and SERGIO CARRÀ,
Dipartimento di Chimica Fisica Applicata, Politecnico di Milano, 20133 Milano, Italy

Synopsis

A comprehensive model of emulsion polymerization batch reactors is presented. The nucleation mechanism via micelles is examined in detail through the introduction of a micellar equilibria model. This allows to predict the influence on the process of the emulsifier amount and type and of the solution ionic strength. A comparison with experimental data of styrene and butadiene polymerization is performed.

INTRODUCTION

Emulsion polymerization is an important process in the manufacture of products such as paints, coatings, adhesive, and others. For this reason in the last few years there have been considerable efforts in developing reliable mathematical models for the simulation of emulsion polymerization reactors. Excellent reviews have been published[1–4] where a detailed discussion and a critical analysis of the proposed models are reported. The most comprehensive mathematical description of emulsion polymerization processes is given in the last one. In it a model is presented, which includes distribution functions of several characteristics of the polymer particles, such as volume, radical number, and polymer chain length. The complexity of the overall model clearly shows the difficulties involved in the design of emulsion polymerization reactors.

The development of the balance equations implies the knowledge of the particle formation mechanisms. In this process an important role is played by the aggregates of emulsifier molecules, which represent the sites of micellar nucleation. The aim of the present paper is to explicitly include equilibria and size distribution of micelles in a simplified comprehensive model of a batch emulsion polymerization reactor. The model has been tested through its application to the simulation of some available experimental data, relative to the styrene and butadiene polymerization reaction. The influence of the emulsifier type and amount and of the solution ionic strength on the micellar nucleation mechanism has been examined in detail.

MATHEMATICAL MODEL

The qualitative picture of the phenomena occurring in a well-stirred batch reactor, which still represents the basic frame of most of the models developed later, has been given by Harkins[5] since 1945. According to this representation, schematically depicted in Figure 1, the material balance equations, which de-

Journal of Applied Polymer Science, Vol. 28, 901–919 (1983)
 CCC 0021-8995/83/030901-19$02.90

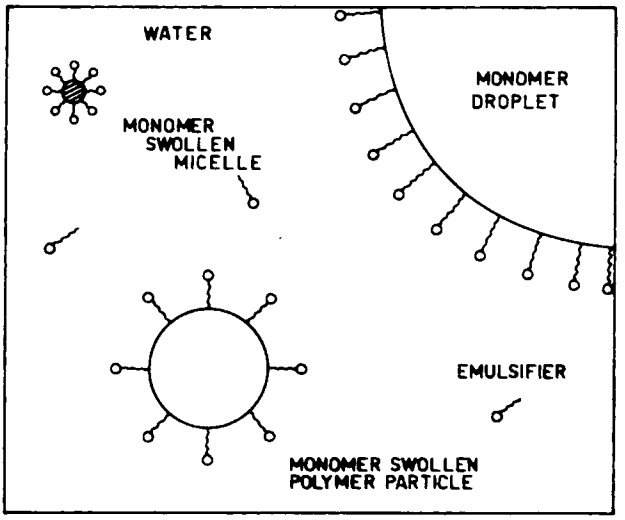

Fig. 1. Physical picture of an emulsion polymerization system.

scribe the transient behavior of the system under examination, have been stated on the basis of the following assumptions: the temperature of the reactor is kept constant throughout the entire process by a suitable temperature control; chain transfer and termination by disproportionation are neglected; all the kinetic rate constants do not depend on the polymer chain length.

Particle Size Distribution Balance

A distribution function of particle volume $f(v,t)$ is introduced, such that $f(v,t)dv$ gives the concentration of polymer particles between the volumes v and $(v + dv)$ at time t. The population balance equation has been applied, in order to describe the evolution of the particle size distribution, as follows:

$$\frac{\partial f}{\partial t} = -\frac{\partial}{\partial v}(g_v f) + r_n \delta(v - v_n) + r_m \delta(v - v_m) + \frac{\beta}{2}\int_0^v f(v - v')f(v')dv' - \beta f(v)\int_0^\infty f(v')\,dv' \quad (1)$$

where $g_v = dv/dt$ is the particle growth rate, r_m and r_n are the particle nucleation rates, via micelles and via aqueous phase oligomer precipitation, respectively, the Dirac function δ indicates that the particle nuclei are characterized by a specific volume v_m or v_n; and β represents the rate coefficient of coalescence.

Various numerical techniques have been proposed so far in the literature[6–9] for solving the integro-differential equation (1). In this work the method of moments according to Hulburt and Katz[6] has been used. It is based on the approximation of the size distribution in terms of series of associated Laguerre polynomials (orthogonalized respect to the Γ-distribution weighting function) truncated at the third term, which is particularly suitable for unimodal distributions of only positive arguments. This allows us to estimate the distribution moment of any order, once the first three μ_0, μ_1, and μ_2 are known. The problem is then reduced to the evaluation of the time evolution of the first three moments

TABLE I
Summary of the Equations Constituting the Solving Procedure

$$\frac{d\mu_0}{dt} = r_n + r_m - \frac{\beta}{2}\mu_0^2$$

$$\frac{d\mu_1}{dt} = \langle g_v f\rangle + r_n v_n + r_m v_m$$

$$\frac{d\mu_2}{dt} = 2\langle g_v f v\rangle + r_n v_n^2 + r_m v_m^2$$

$$f(v,t) = \frac{bc}{a}\frac{1}{\Gamma(b)}\left(\frac{bv}{a}\right)^{b-1}\exp\left(-\frac{bv}{a}\right)$$

$$\mu_n = \langle f v^n\rangle = \frac{\Gamma(n+b)}{\Gamma(b)}c\left(\frac{a}{b}\right)^n, \quad n \neq 0,1,2$$

where

$$\langle X\rangle = \int_0^\infty X\,dv, \quad a = \mu_1/\mu_0, \quad b = \mu_1^2/(\mu_2\mu_0 - \mu_1^2), \quad c = \mu_0$$

of the distribution, which can be obtained directly from eq. (1). All the equations which constitute the solving procedure are summarized in Table I. In the following we will concern about the evaluation of all the quantities appearing in these equations, in particular g_v, r_m, and r_n.

Environmental Balances

The solution polymerization will be described using the following free-radical kinetic scheme:

Initiation:

$$\mathrm{I} \xrightarrow{k_i} 2\mathrm{R}$$

$$\mathrm{R} + \mathrm{M} \xrightarrow{k_{ps}} \mathbf{P}_1$$

Propagation:

$$\mathbf{P}_1 + \mathrm{M} \xrightarrow{k_{ps}} \mathbf{P}_2$$

$$\cdots$$

$$\mathbf{P}_n + \mathrm{M} \xrightarrow{k_{ps}} \mathbf{P}_{n+1}$$

$$\cdots$$

Termination:

$$\mathbf{P}_n + \mathrm{R} \xrightarrow{k_{ts}} \mathrm{P}_n,$$

$$\mathbf{P}_n + \mathbf{P}_m \xrightarrow{k_{ts}} \mathrm{P}_{n+m}, \qquad (n, m = 1, \infty)$$

According to this scheme and to the assumptions summarized at the beginning of this section, the material balances for each species present in the aqueous solution can be derived. Defining the concentrations with reference to the aqueous solution volume, which is constant during the reaction, it follows that

$$\frac{d\mathrm{I}}{dt} = -k_i\,\mathrm{I} \tag{2}$$

$$\frac{d\mathrm{R}}{dt} = 2fk_i\mathrm{I} - k_{ps}\mathrm{MR} - r_m - k_{ts}\mathrm{RP} - k_{mp}\mathrm{RS}_p \tag{3}$$

$$\frac{d\mathbf{P}}{dt} = k_{ps}\mathrm{MR} - k_{ts}\mathbf{P}^2 - k_{ts}\mathbf{PR} - r_n(\mathbf{P}) - k_v\mathbf{P}S_p \tag{4}$$

$$\frac{d\mathrm{P}}{dt} = k_{ts}\mathbf{PR} + \frac{1}{2}k_{ts}\mathbf{P}^2 - r_n(\mathrm{P}) - k_v\mathrm{P}S_p \tag{5}$$

where $\mathbf{P} = \Sigma_{n=1}^{\infty}\mathbf{P}_n$ and $\mathrm{P} = \Sigma_{n=1}^{\infty}\mathrm{P}_n$ represent the total aqueous concentrations of growing and dead polymer chains, respectively. The last term in the rhs of the material balances of species R, P, and **P** represents the disappearance of each species due to polymer particles absorption; S_p represents the total particle surface area, and can be evaluated as $S_p = (36\pi)^{1/3}\mu_{2/3}$, where $\mu_{2/3}$ can be calculated as shown in Table I.

Monomer: A distinction must be made in this case depending on whether or not monomer droplets are present in the aqueous solution.

In the first case, the monomer concentration M is assumed constant and equal to its saturation value M*. Applying then the liquid–liquid equilibrium, it follows that

$$\mathrm{M} = \mathrm{M}^* = \tilde{\rho}_w x_m / K_{\mathrm{eq}} \tag{6}$$

where x_m is the monomer mole fraction in the droplets (usually, $x_m = 1$) and K_{eq} is the liquid–liquid equilibrium constant. This equation clearly derives from the assumption, usually satisfied in practice, that the monomer mass transfer from droplets into the aqueous solution is faster than the polymerization reaction. The total volume of monomer droplets is evaluated through the equation

$$\frac{dV_g}{dt} = -V\frac{\overline{PM}_m}{\rho_m}\left[k_{ps}\mathrm{M}(\mathrm{R} + \mathbf{P}) + \psi(\mathrm{M})\right] \tag{7}$$

The first two terms in brackets represent the monomer consumption due to the polymerization reaction in aqueous solution, while the third represents the consumption of monomer due to the polymerization reaction which takes place in particles.

In the latter case, that is in the absence of monomer droplets, $V_g = 0$. In this case the above-mentioned saturation condition is not valid any more, and the monomer concentration is given by

$$\frac{d\mathrm{M}}{dt} = -\left[k_{ps}\mathrm{M}(\mathrm{R} + \mathbf{P}) + \psi(\mathrm{M})\right] \tag{8}$$

Emulsifier: The material balance of the emulsifier is simply given by the condition $C_{et} = \text{const}$, where C_{et} indicates the initial total concentration of sur-

factant in the system. The distribution of the emulsifier among the different phases present in the reactor will be described shortly.

POLYMER PARTICLE FORMATION

Two different parallel nucleation mechanisms have been taken into consideration. In the former, a radical present in the aqueous phase enters a micelle and starts polymerization. In the latter, the particle formation occurs through precipitation of polymer chains present in solution.

Particle Formation via Micelle

According to this mechanism, the rate of nuclei formation is equal to the rate of radicals absorption into emulsifier micelles, which, according to Gardon,[10] can be expressed as follows:

$$r_m = k_m \mathrm{R} S_m \tag{9}$$

where S_m is the total surface of micelles per unit volume of solution. It can be evaluated from the concentration of micellar emulsifier C_{em}, which is given by

$$C_{em} = C_{et} - C_{ea} - C_{es} \tag{10}$$

In this equation C_{et} is the total emulsifier concentration, C_{ea} represents the emulsifier adsorbed on particles, and C_{es} the free emulsifier dissolved in water.

The concentrations can be evaluated assuming very fast rate transfer and the usual priorities[4] for distribution of the emulsifier; that is: (1) polymer particles; (2) aqueous solution; (3) micelles. It can be reasonably assumed that up to $(C_{et} - C_{ea}) >$ cmc, C_{es} is very close to cmc. The value of C_{ea} can be calculated on the basis of adsorption equilibrium isotherms of emulsifier on polymer particles. This equilibrium can be described by means of the well-known Langmuir isotherm[11]:

$$N_A a_{sp} = \frac{1}{\Gamma_a} = \frac{1 + b_a(C_{es} + C_{em})}{\Gamma_\infty b_a(C_{es} + C_{em})} \tag{11}$$

where a_{sp} is the area occupied by an emulsifier molecule on the polymer surface and Γ_a the emulsifier surface concentration. Thus

$$C_{ea} = S_p / N_A a_{sp} \tag{12}$$

Similarly, S_m is directly related to C_{em} as follows:

$$S_m = a_{sm} N_A C_{em} \tag{13}$$

where a_{sm} is defined as the area occupied by an emulsifier molecule present in a micelle, and it is assumed constant and independent of the emulsifier concentration C_{em}. In previously proposed models[4,12] it was assumed that $a_{sm} = a_{sp}$. Actually, this is a rather poor approximation; in fact, a reliable value of a_{sm} can be obtained only through an analysis of the micelles formation equilibria, by taking into account also the effect of the solution ionic strength. This will be done shortly.

Particle Formation via Precipitation

According to Fitch and Tsai,[13] particle nuclei can be formed by precipitation when the polymer chains in the aqueous solution exceed their solubility limit. The rate of this process can be expressed, as a first approximation, as follows:

$$r_n = k_n(\mathbf{P} + \mathrm{P}) \tag{14}$$

It is worthwhile pointing out that the nucleation rate was originally represented in a different form by Fitch and Tsai,[13] in order to include the competitive effect of absorption by preexisting particles. In the present model this formulation is not necessary, since such effect is already included in the material balances (4) and (5) of the growing and dead polymer chains, respectively.

RATE OF PARTICLE GROWTH

A lumped model is employed to describe the polymerization reaction inside the particles. It implies the use of a mean concentration value of monomer and polymer inside the particle, independent of the radial position within the particle.[14] Since emulsion polymerization reactors are usually well stirred, the monomer inside the particle is assumed in thermodynamic equilibrium with the monomer in the aqueous phase. The monomer volume fraction in the particle can then be evaluated through the following equilibrium condition[15]:

$$(1 - \phi) + \ln\phi + \chi(1 - \phi)^2 - \ln(\mathrm{M/M^*}) = -\frac{2\gamma}{RTr}\frac{\overline{PM}_m}{\rho_m} \tag{15}$$

which represents the balance between the interfacial free energy change and the free energy of mixing. The term on the rhs of eq. (15) accounts for the interfacial free energy contribution, and then it involves the interfacial tension γ and the particle average radius r; χ is the Flory–Huggins constant, used for the evaluation of the mixing free energy of monomer in polymer. Note that the value of χ depends only on the system monomer–polymer, while the interfacial tension γ is a function of the amount of emulsifier adsorbed on the particle surface. In the present work the value of this parameter will be tuned in order to reproduce the experimental values of ϕ measured during the polymerization reaction. In particular it has been assumed the ratio (γ/r) constant with time, according to Gardon.[15]

The particle growth rate g_v is given by the sum of two terms:

$$g_v = \frac{dv}{dt} = r_p \frac{\overline{PM}_m}{\rho_p} v + \frac{d}{dt}(\phi v) \tag{16}$$

where the polymerization rate r_p is given by

$$r_p = k_p \frac{Q}{N_A v}\frac{\phi\rho_m}{\overline{PM}_m} \tag{17}$$

and Q indicates the average number of radicals per particle.

It is now necessary to evaluate the number of radicals per particle as a function of the particle volume. This has been done by Stockmayer[16] in the case of negligible radicals desorption from particles and applying the quasi-steady-state approximation to the radical concentration. This last approximation is ac-

ceptable when the following condition is satisifed[3]:

$$\frac{k_t}{k_p} \gg \frac{\phi}{4(1-\phi)} \frac{\rho_m}{\rho_p} \tag{18}$$

Equation (18) holds for various systems of practical import, including those examined in detail in the following sections of this work. It is worthwhile pointing out that other expressions of the same type as Stockmayer one are available[3,17] for systems where the two conditions mentioned above are not satisfied.

In order to introduce the Stockmayer equation in the above-developed model, it is necessary to rewrite it in a different form, more suitable for the application of the method of moments. In particular, a polynomial expression has been developed:

$$Q = 0.5 + a_1\gamma^{3/5} + a_2\gamma^{6/5} + a_3\gamma^{9/5} + a_4\gamma^{12/5} \tag{19}$$

where $a_1 = 4.7572 \times 10^{-1}$, $a_2 = -3.9368 \times 10^{-3}$, $a_3 = 4.0954 \times 10^{-5}$, and $a_4 = -1.6817 \times 10^{-7}$. This expression reproduces the Stockmayer equation results with an error which never exceeds 10%. The variable γ in eq. (19) is similar to the one used by Stockmayer, although here refers only to the class of particles with volume v. In particular,

$$\gamma = \frac{\rho_a v}{N_v k_t} N_A^2 \tag{20}$$

where $N_v = f(v,t)dv$ and ρ_a represents the rate of radical absorption in the N_v particles, given by

$$\rho_a = (k_{mp}\mathrm{R} + k_v\mathbf{P})(36\pi)^{1/3} v^{2/3} N_v \tag{21}$$

Substituting eq. (21) in eq. (20) gives

$$\gamma = \bar{K} v^{5/3} \tag{22}$$

where

$$\bar{K} = (k_{mp}\mathrm{R} + k_v\mathbf{P})(36\pi)^{1/3} N_A^2/k_t \tag{23}$$

Using eqs. (16), (17), and (19) it is now possible to explicitly calculate the integrals appearing in the solving equations reported in Table I, and the total monomer consumption rate in the polymer particles $\psi(\mathrm{M})$, appearing in eqs. (7) and (8). The following equations are obtained:

$$\int_0^\infty g_v f v^j dv = \frac{1}{1-\phi}\left(\frac{\rho_m}{\rho_p} k_p \frac{\phi}{N_A} \chi_{j+1} + \frac{d\phi}{dt} \mu_{j+1}\right), \quad j = 0,1 \tag{24}$$

$$\chi_{j+1} = 0.5\,\mu_j + a_1\bar{K}^{3/5}\mu_{j+1} + a_2\bar{K}^{6/5}\mu_{j+2} + a_3\bar{K}^{9/5}\mu_{j+3} + a_4\bar{K}^{12/5}\mu_{j+4} \tag{25}$$

$$\psi(\mathrm{M}) = \frac{\rho_m}{\bar{P}\bar{M}_m}\left[k_p \frac{\phi}{N_A} \chi_1 \left(1 + \frac{\rho_m}{\rho_p} \frac{\phi}{1-\phi}\right) + \frac{\mu_1}{1-\phi} \frac{d\phi}{dt}\right] \tag{26}$$

MICELLAR EQUILIBRIA IN AQUEOUS SOLUTION

In the subsection Particle Formation via Micelle it has been pointed out that the description of particle nucleation via micelles through eq. (9) implies the

correct evaluation of the total micellar surface S_m. This possibility is offered by a recently proposed model of micelle formation,[18] in which the distribution of micelle sizes is expressed as a function of the total concentration of emulsifier in the aqueous solution $C_e = C_{em} + C_{es}$. We will here summarize the basic features of this model, in the case of emulsifier molecules which can be schematized as a hydrophilic head group (either ionic or nonionic) with a hydrocarbon tail. The shape of the micellar aggregates is assumed spherical. Discrepancies from such assumptions have been considered elsewhere.[19]

The examined micellar equilibria model is essentially based on the following equations:

$$\frac{N_g}{N_{\text{tot}}} = \left(\frac{N_e}{N_{\text{tot}}}\right)^g \exp\left(-\frac{g\Delta\mu_{eb} + \mu_g}{kT}\right), \quad g = 2, 3, \ldots, \infty \tag{27}$$

$$N_{\text{tot}} = N_s + N_e + \sum_{g=2}^{\infty} gN_g \tag{28}$$

where N_g is the number of micelles containing g molecules of emulsifier, N_e the number of emulsifier molecules dissolved in water, N_s the number of solvent molecules, and N_{tot} the total number of emulsifier molecules present in the aqueous solution (excluding those adsorbed on polymer particles). Equations (27) represent the equilibrium condition, i.e., that the system free energy is minimum, and eq. (28) is simply the material balance of the free emulsifier in the aqueous solution. The term $\Delta\mu_{eb}$ represents the standard free energy change in transferring an emulsifier molecule from the dilute aqueous phase to the hydrocarbon phase of the micellar core. According to Tanford,[20] it can be evaluated as follows:

$$\frac{\Delta\mu_{eb}}{kT} = \frac{S + J(n_c - 1)}{RT} \tag{29}$$

where the parameter S, which depends on the specificity of the head group, is assumed equal to -2000 cal/mol; the term J, which depends on the head group character, is assumed equal to -420 cal/mol; n_c is the number of carbon atoms in the hydrocarbon tail of the emulsifier. The quantity μ_g is the contribution to the standard free energy of formation of micelles which includes the attractive hydrophobic bonding between hydrocarbon tails of emulsifier and the repulsive interaction between their hydrophilic head groups. It can be evaluated as follows[20]:

$$\frac{\mu_g}{kT} = \frac{25(A - 21)g}{RT} + \frac{\alpha g}{ART} \tag{30}$$

where A $(= 4\pi r_0^2/g)$ is the surface area per emulsifier molecule in an aggregate of size g and radius r_0 and α is a parameter relative to the repulsive interaction between the emulsifier head groups.

In eq. (30) two contributions are taken into account: the interaction energy between the micellar hydrophobic core and water, which tends to decrease the aggregate size; the interaction energy between the head groups of the emulsifier molecules present in the aggregate, which tends to increase its size.

The conflict between these two effects determines the equilibrium volume of the micellar aggregates.

As above mentioned, all the parameters appearing in the model can be evaluated on the basis of semiempirical correlation,[20] with the only exception of the interaction parameter α. A naive way to evaluate it is to consider the work necessary to locate an electrical charge on a spherical surface, equal to the area occupied by an emulsifier molecule on the micelle, a_{sm}. The calculation of α is then performed by using the charging process of the Debye–Hückel theory. This simplified approach is unfortunately not valid, since the high charge density generated by the head groups leads to substantial charge neutralization by counterions.[21] Therefore, in the present work, the parameter α has been adjusted in order to force the model to reproduce the experimental values of cmc for various emulsifiers.

The use of eqs. (27) and (28) allows to evaluate, for a given amount of emulsifier (N_{tot}) and solvent (N_s), the entire micellar distribution (i.e., N_g for $g = 2, 3, \ldots, \infty$) and the amount of emulsifier dissolved in water in a molecular form, N_e. The micellar distribution exhibits an inflection point at a specific value of the free emulsifier concentration C_e, which constitutes a close lower bound of the cmc. It is worthwhile pointing out that, since the interaction parameter α depends on the emulsifier head group type and on the solution ionic strength I its calibration must be repeated for each emulsifier and for each value of I.

The above described model can now be used for the evaluation of a_{sm}, which through eqs. (9) and (13) affects the nucleation rate via micelles. As an illustrative example, sodium lauryl sulphate (SLS) will be considered.

First, the micellar distribution function has been evaluated for increasing values of the free emulsifier concentration C_e. From this, the average micellar volume v_m and the total micellar surface S_m can be derived. The obtained results are shown in Figure 2 for the case of solution ionic strength equal to 0.0028 mol/L. It appears that, while the value of v_m tends to reach a constant value

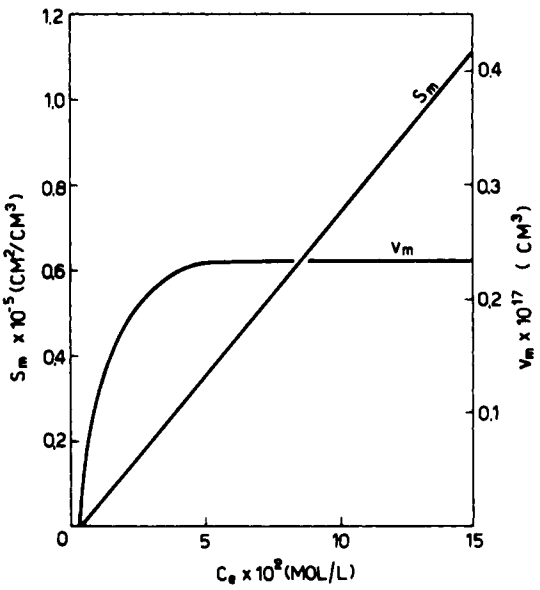

Fig. 2. Calculated values of total micellar surface S_m and micellar volume v_m as a function of emulsifier (SLS) concentration. $T = 60°C$; $I = 2.8 \times 10^{-3}$ mol/L; cmc = 3.1×10^{-3} mol/L.

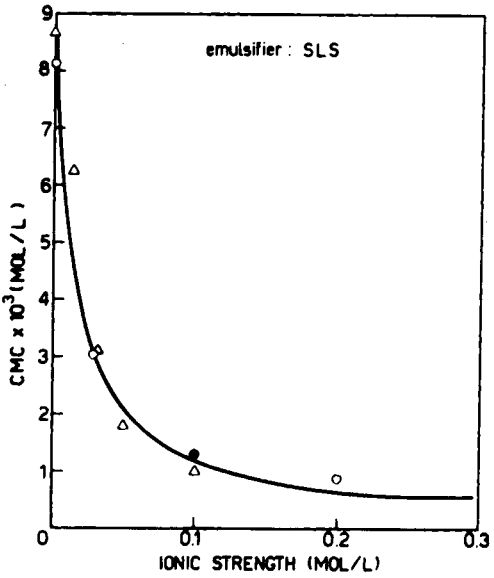

Fig. 3. Experimental values of cmc as a function of the solution ionic strength. Data sources: (○) Elworthy et al.[38]; (●) Brodnyan and Lloyd Kelley[11]; (△) Piirma and Chen.[39]

at large C_e, the value of S_m increases almost linearly. This finding is due to the influence of the micellar distribution function. From eq. (13) it follows that the value of a_{sm} can be assumed approximately constant, as is usually done in all previous treatments. Note also that, for the case under consideration (SLS, styrene) a_{sm} = 13.4 Å^2/molecule, while a_{sp} = 35 ÷ 50 Å^2/molecule, as reported in the literature.[11,22,23] Therefore, these two quantities must be kept separate in emulsion polymerization models.

The influence of the solution ionic strength at constant free emulsifier con-

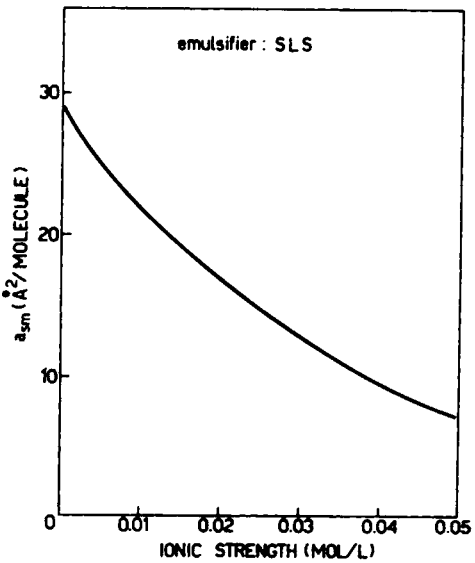

Fig. 4. Calculated values of a_{sm} as a function of the solution ionic strength. T = 60°C.

centration has been also investigated. The values of the interaction parameter, as a function of I, has been calculated through calibration of the model on the correspondent experimental values of cmc, shown in Figure 3. Note that the experimental data of Figure 3 have been obtained at $T = 20 \div 25°C$. In the following part of this work, the dependence of cmc on temperature has been neglected. Through the same procedure previously outlined, the values of a_{sm} as a function of I, shown in Figure 4, have been calculated. As expected, the effect of the solution ionic strength on the micellar surface is quite significant and for a given amount of emulsifier, it decreases for increasing values of I. The role of this phenomenon in emulsion polymerization will be examined in detail in the next section.

COMPARISON WITH EXPERIMENTAL DATA

The previously developed model has been used to simulate two different emulsion polymerization processes: polystyrene and polybutadiene. The aim is to verify the model reliability with respect to three aspects of the emulsion polymerization process:

(1) effect of the emulsifier concentration on reaction and nucleation rates;

(2) effect of the emulsifier type on the polymerization rate;

(3) influence of the aqueous solution ionic strength on the conversion and the particle number.

In all the above-mentioned points the micellar equilibria model is expected to play an important role. Suitable experimental data are taken from the literature for comparison with the model results.

All the parameters appearing in the model have been evaluated from experiments reported in the literature, which do not involve emulsion polymerization kinetics. A summary of the numerical values of each parameter and their source is reported in Tables II and III for styrene and butadiene, respectively. The only exceptions are the mass transfer rate constant of radicals in micelles k_m and the homogeneous nucleation rate constant k_n for styrene polymerization. For the butadiene polymerization, again two parameters are not defined in the literature: k_m and the termination rate constant in polymer particle, k_t. The evaluation of such parameters has been performed in both cases through a fitting procedure with the experimental values relative to one batch emulsion polymerization experiment. In particular, the data reported by Harada et al.[22] and Kolthoff et al.[24] have been used for styrene and butadiene, respectively.

It is worthwhile pointing out that the effect of particle coalescence has been neglected (i.e., $\beta = 0$), due to the low stirring speed and the large emulsifier concentration; this has been experimentally verified by Nomura et al.[25] for the styrene polymerization. In the case of butadiene polymerization the emulsifier concentration was large in all the examined runs, so that also the homogeneous nucleation mechanism can be neglected (i.e., $k_n = 0$).

The gel effect has been accounted for the styrene case, using the following expression for the termination rate constant k_t as a function of the monomer conversion X[26]

$$k_t = k_t^0 \exp\left[-2(BX + CX^2 + DX^3)\right]$$

TABLE II
Parameter Values Employed in Simulation of Emulsion Polymerization of Styrene (Figs. 5 and 7)

Parameter	Source	Numerical value
K_{eq}	32	1.18×10^4 in Fig. 7 1.51×10^4 in Fig. 5
χ	15,22	0.43
γ (dyn/cm)		~30
Γ_∞ (mol/cm^2)	22	4.74×10^{-10}
b_a (cm^3/mol)	23	8×10^6
cmc (n_c = 12) (cm^3/mol)	22,30	9.0×10^{-6} in Fig. 7 1.7×10^{-6} in Fig. 5
a_{sm} (Å^2/molecule)	Calculated through micellar equilibrium model	29.0 in Fig. 7 9.2 in Fig. 5
k_p	—	$= k_{ps}$
k_t^0 (cm^3/mol·s)	33	5.0×10^{10} in Fig. 7 2.9×10^{10} in Fig. 5
B		$3.57\text{–}5.05 \times 10^{-3}\ T$
C [T (°K)]	26	$9.56\text{–}1.76 \times 10^{-2}\ T$
D		$-3.03 + 7.85 \times 10^{-3}\ T$
k_{ps} (cm^3/mol·s)	34	$2.12 \times 10^9 \exp(-5900/RT)$
k_{ts} (cm^3/mol·s)	34	$2.61 \times 10^{11} \exp(-524/RT)$
k_{mp} (cm/s)	—	$= k_m$
k_v (cm/s)	—	$= k_m$
k_m (cm/s)	By fitting	1.5×10^{-5} in Fig. 7 5.0×10^{-5} in Fig. 5
k_n (1/s)	By fitting	0.0 in Fig. 7 2.0×10^{-2} in Fig. 5

where the values of the parameters k_t^0, B, C, and D have been reported in Table II. On the other hand, the gel effect has been neglected for butadiene, since the

TABLE III
Parameter Values Employed in the Simulation of Emulsion Polymerization of Butadiene (Fig. 6)

Parameter	Source	Numerical value
K_{eq}	35	1.80×10^2
K	35	1.56×10^3
Γ_∞ (mol/cm^2)	29	6.20×10^{-10}
b_a (cm^3/mol)		2.33×10^6
cmc (mol/cm^3)	35	$\sim 1 \times 10^{-7}$
a_{sm} (Å^2/molecule)	Calculated through micellar equilibrium model	24.7
k_p	—	$= k_{ps}$
k_t (cm^3/mol·s)	By fitting	1.25×10^6
k_{ps} (cm^3/mol·s)	36	$1.20 \times 10^{11} \exp(-9300/RT)$
k_{ts} (cm^3/mol·s)	36	1.0×10^{11}
k_i (1/s)	37	$5.61 \times 10^{16} \exp(-33500/RT)$
k_{mp} (cm/s)	—	$= k_m$
k_v (cm/s)	—	$= k_m$
k_m (cm/s)	By fitting	1.5×10^{-7}
k_n (1/s)	—	0

available experimental data were not sufficient for its evaluation. An average constant value of k_t will then be estimated in the following.

The adsorption isotherm of the emulsifier on particles have been evaluated through limited experimental data. For adsorption of sodium lauryl sulphate (SLS) on styrene, we have considered the value provided by Nomura et al.[23] ($a_{sp} \simeq 35$ Å^2/molecule at C_e = cmc); b_a was calculated assuming $\Gamma_\infty \simeq \Gamma_a$ evaluated at the cmc. There is a very poor agreement between the isotherm so obtained and experimental isotherms reported in literature for the same system.[11,27] Due to the scattering in the experimental data themselves, the isotherm reported by Harada et al. was used. For adsorption of potassium laurate (PL) on butadiene, it was assumed $\Gamma_\infty = (1/N_A a_{sp})$ with a_{sp} obtained from the literature.[28,29] No other experimental data were found; b_a was calculated through the empirical rule Γ_a at the cmc = $0.7\Gamma_\infty$.

Finally, the parameter values needed in eq. (15) have been found in literature only in the styrene case. So, for butadiene, the oversimplified linear equilibrium relation

$$\phi = KM\frac{\overline{PM}_m}{\rho_m}$$

has been used.

In Figures 5 and 6 are shown the calculated and experimental values of conversion vs. time, for various emulsifier concentrations, in the case of styrene and butadiene polymerization, respectively. The two adjustable parameters have been calibrated in both cases using the conversion-time experimental values relative to the intermediate emulsifier concentration. Subsequently, the other curves have been obtained using the model with the same parameter values. In Table IV the experimental and calculated values of particle number, relative to the styrene polymerization runs shown in Figure 5, are reported. As mentioned above, both the homogeneous and the micellar nucleation mechanism

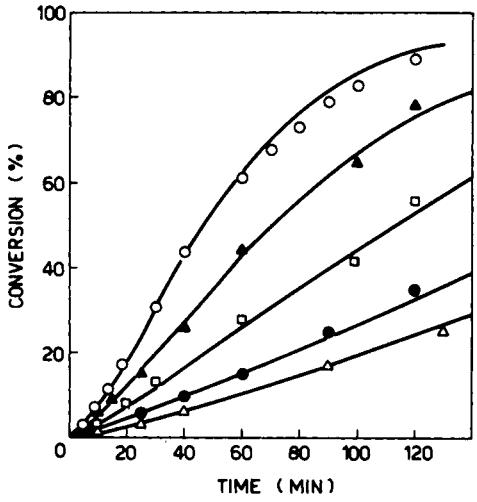

Fig. 5. Conversion-time curves for styrene polymerization at various emulsifier concentrations. Amount of water: 1000 cm^3; amount of monomer: 572 cm^3; initial concentration of initiator ($K_2S_2O_8$): 4.6×10^{-6} mol/cm^3; initial concentration of emulsifier (SLS) (g/L): (○) 25.00, (▲) 12.50, (□) 6.25, (●) 3.13, (△) 1.88; T = 50°C.

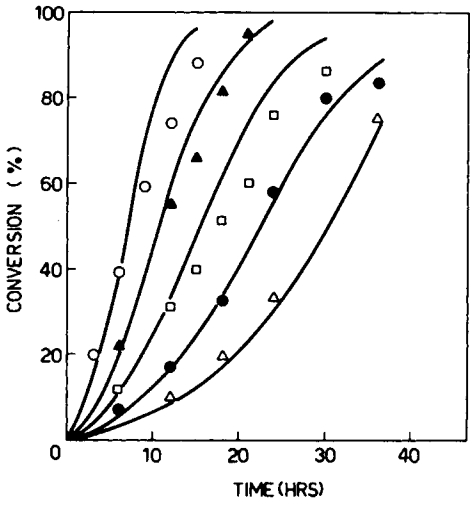

Fig. 6. Conversion-time curves for butadiene polymerization at various emulsifier concentrations. Amount of water: 182.2 cm^3; amount of monomer: 171.9 cm^3; initial concentration of initiator ($K_2S_2O_8$): 6.09×10^{-6} mol/cm^3; initial concentration of emulsifier (PL) (g/L): (○) 53.40, (▲) 26.70, (□) 13.40, (●) 6.68, (△) 3.34; $T = 50°C$.

are active in this case. So, with illustrative purposes, in Table IV are reported also the particle number values which are obtained from the model neglecting the homogeneous nucleation mechanism (i.e., $k_n = 0$). It appears that the effect of homogeneous nucleation is significant at low emulsifier concentration ($C_{et} \simeq$ cmc), while it vanishes at large emulsifier concentration, where the particle number produced by the micellar mechanism is large. This is the case of all the examined runs relative to butadiene polymerization, where the homogeneous nucleation has then been neglected.

The effect of the emulsifier type has been investigated through the micellar equilibria model. Experimental data of Al-Shahib and Dunn,[30] about styrene emulsion polymerization, have been used. Three sodium alkyl sulphates, with an hydrocarbon tail of n_c = 12, 14, and 18 respectively, have been considered. The value of the parameter α, which is independent of the hydrocarbon tail length, has been tuned on the experimental cmc values of SLS (n_c = 12).[30] In Figure 7 the total micellar surface S_m as a function of the total free emulsifier concentration C_e is shown for the three emulsifiers under consideration. It

TABLE IV
Comparison between Experimental and Calculated Values of Particle Number (Styrene Polymerization; Fig. 5)

Emulsifier concn (g/L)	Particle number $\times 10^{-14}$ (1/cm^3)		
	Experimental values	Calculated	
		$k_n = 0$	$k_n = 0.02$
25.00	10.0	10.18	10.20
12.50	6.0	6.20	6.30
6.25	4.0	3.50	3.70
3.13	2.2	1.80	2.30
1.88	1.6	1.00	1.80

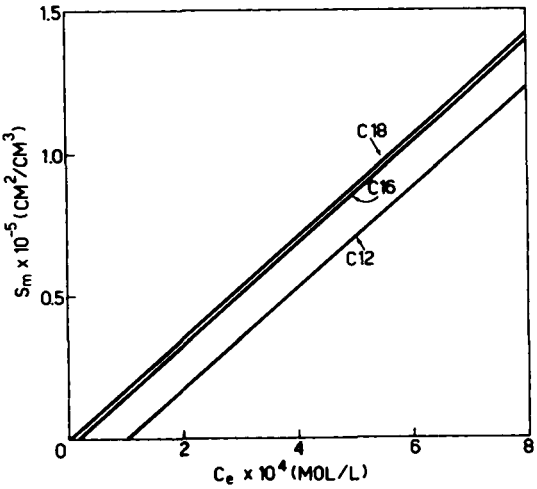

Fig. 7. Calculated values of micellar surface as a function of emulsifier concentration.

appears that three straight lines with the same slope are obtained. As expected,[28] it can be concluded that the same value of a_{sm} can be used for the three emulsifiers. The cmc values of the C_{14} and C_{18} emulsifiers, predicted by the model are compared with the experimental ones[30] in Figure 8. In the same figure the conversion vs. time curves are also shown together with the experimental values. On the whole it can be concluded that the effect of hydrocarbon tail length, in

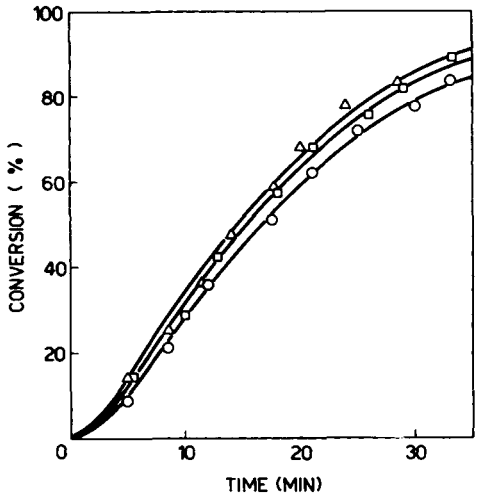

Fig. 8. Conversion-time curves for styrene polymerization with various surfactants (alkyl sulphates with different chain lengths). Amount of water: 212.0 cm^3; amount of monomer: 80.0 cm^3; initial concentration of initiator ($K_2S_2O_8$): 7.4×10^{-6} mol/cm^3; initial concentration of the various emulsifiers: 60×10^{-5} mol/cm^3; $T = 60°C$. cmc $\times 10^3$ (mol/L):

	Calcd	Exptl
(○) C12	8.94	9.00
(□) C14	2.50	2.40
(△) C18	0.20	0.16

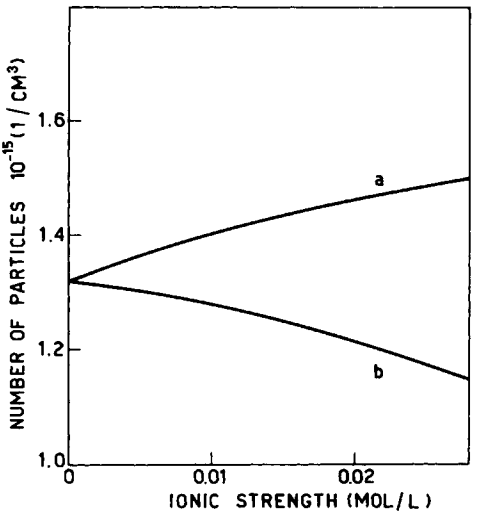

Fig. 9. Polymer particle number as a function of the solution ionic strength for styrene polymerization. Amount of water: 212.0 cm^3; amount of monomer: 80.0 cm^3; initial concentration of initiator ($K_2S_2O_8$): 7.4×10^{-6} mol/cm^3; initial concentration of emulsifier (SLS): 5.0×10^{-5} mol/cm^3; $T = 60°C$.

linear emulsifiers, is reasonably well predicted by the model. It is worthwhile pointing out that in the calculations above reported all the emulsifiers have been assumed to follow the same adsorption isotherm on polymer particles. In particular, the isotherm relative to SLS ($n_c = 12$) was considered. Although this assumption has not been verified experimentally, data reported in literature[28] relatively to $n_c = 12$ and $n_c = 14$ confirm it.

Finally the effect of the solution ionic strength on the process has been investigated. As shown in Figures 3 and 4, the ionic strength I affects both the cmc and the emulsifier molecular surface in micelle a_{sm}. The aim here is to show how this affects the final number of polymer particles, N. In Figure 9 the calculated values of N as a function of I are shown for the recipe specified in the caption of the figure. Two different situations have been considered: (a) the only variation of cmc with I has been considered, while a_{sm} has been kept constant; (b) the influence of I on both cmc and a_{sm} has been taken into account. From the data shown in Figure 9 it appears that in case (a) the polymer particle number increases for increasing values of I. This is due to the cmc decrease, shown in Figure 3, which increases the amount of free emulsifier available for particle nucleation via micelles. However, in case (b) increasing values of I lead also to smaller values of a_{sm}. Therefore, although the total amount of emulsifier available for micelles formation increases, the total micellar surface S_m decreases. This justifies the decrease of the polymer particle number with increasing values of the ionic strength.

It is worthwhile pointing out that the effect of the ionic strength on the emulsifier adsorption of polymer particles and on the particle coalescence rate has been neglected in the above-illustrated calculations. This assumption can be quite significant specifically at low emulsifier concentration, where the coalescence rate (i.e., β) increases rapidly with increasing values of the ionic strength. However, experimental data have been reported by Al-Shabib and

Dunn,[31] which qualitatively confirm the trend of curve (b) in Figure 9 for the batch emulsion polymerization of methylmethacrylate. Since in this case, due to the large amount of emulsifier used, the coalescence effect, as observed by the authors,[31] was negligible, the variation of the micellar size can be regarded as the principle cause of this trend.

The financial support of the Italian Consiglio Nazionale delle Ricerche (Progetto Finalizzato Chimica Fine e Secondaria) is gratefully acknowledged.

APPENDIX: NOMENCLATURE

a_{sm}	molecular surface of emulsifier in a micelle
a_{sp}	molecular surface of emulsifier adsorbed on a polymer particle
b_a	adsorption equilibrium constant
C_e	total emulsifier concentration in the aqueous phase, ($C_{es} + C_{em}$)
C_{et}	total emulsifier concentration per unit volume of aqueous solution
C_{ea}	emulsifier concentration adsorbed on polymer particles
C_{em}	emulsifier concentration in micellar aggregates
C_{es}	emulsifier concentration dissolved in water
cmc	critical micelle concentration
f	efficiency of initiator decomposition (= 0.5)
$f(v,t)$	particle volume distribution function
g	number of emulsifier molecules in a micelle
g_v	particle volume growth rate
I	aqueous solution ionic strength
I	initiator concentration per unit volume of aqueous solution
k	Boltzman's constant
k_i	decomposition rate constant of the initiator
k_m	mass transfer rate constant of radicals in micelles
k_{mp}	mass transfer rate constant of radicals in particles
k_n	homogeneous nucleation rate constant
k_p	polymerization rate constant in particle
k_{ps}	polymerization rate constant in aqueous solution
k_t	termination rate constant in particle
k_{ts}	termination rate constant in aqueous solution
k_v	mass transfer rate constant of polymer chains in particles
K	equilibrium constant between monomer in particle and monomer dissolved in water
K_{eq}	equilibrium constant between monomer in droplets and monomer dissolved in water
M	monomer concentration per unit volume of aqueous solution
M*	monomer concentration per unit volume of aqueous solution at saturation
n_c	number of carbon atoms in the emulsifier alkyl chain
N	number of particles per unit volume of aqueous solution
N_A	Avogadro number
P	total concentration of dead polymer chains per unit volume of aqueous solution
P	total concentration of growing polymer chains per unit volume of aqueous solution
P_n	concentration of dead polymer chains constituted by n monomeric units
$\mathbf{P}_n$	concentration of growing polymer chains constituted by n monomeric units
$\overline{PM}_m$	monomer molecular weight
Q	average number of radicals per particle
r	particle radius
r_m	nucleation rate via micelles
r_n	homogeneous nucleation rate
R	radical concentration per unit volume of aqueous solution
R	ideal gas constant
S_m	total surface of micelles per unit volume of aqueous solution
S_p	total surface of polymer particles per unit volume of aqueous solution
t	time

T	temperature
v	particle volume
V_g	total volume of monomer droplets
v_m	micellar volume
v_n	volume of a precipitated nucleus
V	total volume of aqueous solution
x_m	monomer mole fraction in droplets
X	monomer conversion

Greek Letters

β	coalescence effectiveness
Γ_a	surface concentration of emulsifier on the polymer particles
Γ_∞	surface concentration of emulsifier on the polymer particle at saturation
$\Gamma(x)$	gamma function
γ	interfacial tension between particles and solution
μ_n	distribution moment of n-th order
ρ_m	monomer density
ρ_p	polimer density
$\tilde{\rho}_w$	molar density of water
ρ_a	rate of radical absorption in polymer particles
ϕ	monomer volume fraction in polymer
χ	Flory–Huggins constant

References

1. H. Gerrens, *Fortschr. Hochpolym. Forsch.*, **1**, 234 (1969).
2. B. M. E. Van der Hoff, *Solvent Properties of Surfactant Solutions*, K. Shinoda, Ed., Marcel Dekker, New York, 1967.
3. J. Ugelstad and F. R. Hansen, *Rubber Chem. Technol.*, **49**, 536 (1976).
4. K. W. Min and H. W. Ray, *J. Macromol. Sci., Rev. Macromol. Chem.*, **C11**, 177 (1974).
5. W. D. Harkins, *J. Chem. Phys.*, **13**, 381 (1945); *J. Am. Chem. Soc.*, **69**, 1428 (1947); *J. Polym. Sci.*, **5**, 217 (1950).
6. H. M. Hulburt and S. Katz, *Chem. Eng. Sci.*, **19**, 555 (1964).
7. S. K. Bhatia and D. D. Perlmutter, *AIChE J.*, **25**, 298 (1979).
8. P. N. Singh and D. Ramkrishna, *Comp. Chem. Eng.*, **1**, 23 (1977).
9. G. Ley and H. Gerrens, *Macromol. Chem.*, **175**, 563 (1974).
10. J. L. Gardon, *J. Polym. Sci., A-1*, **6**, 623 (1968).
11. J. G. Brodnyan and E. Lloyd Kelley, *J. Polym. Sci., C*, **27**, 263 (1969).
12. J. L. Gardon, *J. Polym. Sci., A-1*, **6**, 643 (1968).
13. R. M. Fitch and C. H. Tsai, *Polymer Colloids*, R. M. Fitch, Ed., Plenum, New York, 1971.
14. J. L. Gardon, *J. Polym. Sci.*, **11**, 241 (1973).
15. J. L. Gardon, *J. Polym. Sci., A-1*, **6**, 2859 (1968).
16. W. H. Stockmayer, *J. Polym. Sci.*, **24**, 314 (1957).
17. D. C. Blackley, "Emulsion Polymers and Emulsion Polymerization," ACS Symposium Series 165, American Chemical Society, Washington, D.C., 1981, p. 437.
18. E. Ruckenstein and R. Nagarajan, *J. Phys. Chem.*, **79**, 2822 (1975).
19. E. Ruckenstein and R. Nagarajan, *Micellization, Solubilization and Microemulsion*, K. L. Mittal, Ed., Plenum, New York, 1977, Vol. 1, p. 133.
20. C. Tanford, *J. Phys. Chem.*, **78**, 2469 (1974).
21. G. Gunnarsson, B. Jönsson, and H. Wennerström, *J. Phys. Chem.*, **84**, 3114 (1980).
22. M. Harada, M. Nomura, H. Kojima, W. Eguchi, and S. Nagata, *J. Appl. Polym. Sci.*, **16**, 811 (1972).
23. M. Nomura, H. Kojima, M. Harada, W. Eguchi, and S. Nagata, *J. Appl. Polym. Sci.*, **15**, 675 (1971).
24. I. M. Kolthoff, E. J. Meehan, and C. W. Carr, *J. Polym. Sci.*, **6**, 73 (1950).
25. M. Nomura, M. Harada, W. Eguchi, and S. Nagata, *J. Appl. Polym. Sci.*, **16**, 835 (1972).

26. A. W. Hui and A. E. Hamielec, *J. Appl. Polym. Sci.*, **16,** 749 (1972).
27. V. I. Yeliseyeva and A. V. Zuikov, *Emulsion Polymerization*, ACS Symposium Series 24, American Chemical Society, Washington, D.C., 1976, p. 62.
28. J. Bandrup and H. Immergut, *Polymer Handbook*, Interscience, New York, 1967.
29. S. H. Maron, M. E. Elder, and I. N. Ulevitch, *J. Colloid Sci.*, **9,** 89 (1954).
30. W. A. G. R. Al-Shahib and A. S. Dunn, *J. Polym. Sci.*, **16,** 677 (1978).
31. W. A. G. R. Al-Shahib and A. S. Dunn, *Br. Polym. J.*, **10,** 137 (1978).
32. F. A. Bovey and I. M. Kolthoff, *J. Polym. Sci.*, **5,** 487 (1950).
33. N. Friis and A. E. Hamielec, *J. Polym. Sci.*, **11,** 3341 (1973).
34. S. Olivè and G. H. Olivè, *Makromol. Chem.*, **37,** 71 (1960).
35. F. A. Bovey, I. M. Kolthoff, A. I. Medalia, and E. J. Meehan, *Emulsion Polymerization*, Interscience, New York, 1955.
36. M. Morton and P. P. Salatiello, *J. Polym. Sci.*, **6,** 225 (1951).
37. I. M. Kolthoff and I. R. Miller, *J. Am. Chem. Soc.*, **73,** 3055 (1951).
38. P. H. Elworthy, A. T. Florence, and C. B. Mac Farlane, *Solubilization by Surface Active Agents*, Chapman and Hall, London, 1968.
39. I. Piirma and Shih-R. Chen, *J. Colloid Interface Sci.*, **5,** 487 (1950).

Received April 30, 1982
Accepted October 14, 1982